



Noncanonical NF-{kappa}B Activation by the Oncoprotein Tio Occurs Through a Nonconserved TRAF3-Binding Motif

Sarah Jill de Jong, Jens-Christian Albrecht, Fabian Giehler, Arnd Kieser, Heinrich Sticht and Brigitte Biesinger (23 April 2013)

Science Signaling 6 (272), ra27. [DOI: 10.1126/scisignal.2003309]

The following resources related to this article are available online at http://stke.sciencemag.org.
This information is current as of 24 April 2013.

Article Tools Visit the online version of this article to access the personalization and article tools:

http://stke.sciencemag.org/cgi/content/full/sigtrans;6/272/ra27

Supplemental "Supplementary Materials"

Materials http://stke.sciencemag.org/cgi/content/full/sigtrans;6/272/ra27/DC1

Related Content The editors suggest related resources on *Science*'s sites:

http://stke.sciencemag.org/cgi/content/abstract/sigtrans;5/246/ra75 http://stke.sciencemag.org/cgi/content/abstract/sigtrans;3/123/ra41

References This article cites 47 articles, 21 of which can be accessed for free:

http://stke.sciencemag.org/cgi/content/full/sigtrans;6/272/ra27#otherarticles

Glossary Look up definitions for abbreviations and terms found in this article:

http://stke.sciencemag.org/glossary/

Permissions Obtain information about reproducing this article:

http://www.sciencemag.org/about/permissions.dtl

NF-KB SIGNALING

Noncanonical NF-κB Activation by the Oncoprotein Tio Occurs Through a Nonconserved TRAF3-Binding Motif

Sarah Jill de Jong,¹* Jens-Christian Albrecht,¹ Fabian Giehler,² Arnd Kieser,² Heinrich Sticht,³ Brigitte Biesinger^{1†}

Members of the nuclear factor κB (NF- κB) family of transcription factors regulate many cellular functions. Activation of NF- κB signaling is commonly classified as occurring through canonical or noncanonical pathways. Most NF- κB -inducing stimuli, including the viral oncoprotein Tio, lead to a concerted activation of both NF- κB pathways; however, extensive crosstalk at multiple levels between these signaling cascades restricts the ability to discriminate between the canonical and the noncanonical effects. We showed that noncanonical NF- κB activation by Tio depends on a distinct sequence motif that directly recruits tumor necrosis factor receptor–associated factor 3 (TRAF3). Through its TRAF3-binding motif, Tio triggered a ubiquitin-independent depletion of TRAF3 from the cytosol, which prevented TRAF3 from inhibiting signaling through the noncanonical NF- κB cascade. Furthermore, the Tio-TRAF3 interaction did not affect components of the canonical NF- κB signaling pathway or the expression of target genes; thus, Tio induced noncanonical NF- κB independently of crosstalk with the canonical pathway. Together, these data identify a distinct molecular mechanism of noncanonical NF- κB activation that should enable studies into the particular functions of this pathway.

INTRODUCTION

The nuclear factor κB (NF- κB) family of transcription factors are versatile regulators of lymphoid cell function. They guide lymphoid cell development, proliferation, and survival and thereby control innate and adaptive immune responses. Given these pleiotropic functions, the induction of NF- κB responses relies on a precisely tuned balance between activating and inhibitory signals and hence is extremely vulnerable to perturbations. Aberrant and excessive NF- κB activity is detrimental and may lead to oncogenic lymphocyte transformation. Therefore, it is not surprising that constitutive NF- κB signaling has been described as a key pathological feature in various lymphoid malignancies (1, 2). Lymphotropic tumor viruses have evolved multiple strategies to target NF- κB signaling to enable sustained viral replication, cellular growth, and evasion of apoptosis, which finally cumulate in oncogenic transformation (3–6). The viral oncoproteins that mediate this transforming phenotype can thus serve as excellent tools to study NF- κB signaling.

At the molecular level, two distinct routes to NF- κ B activation are described: the canonical (or classical) and the noncanonical (or alternative) pathways (Fig. 1). Canonical NF- κ B responses are elicited by a broad range of stimuli. Typically, receptor ligation induces the recruitment of adaptor molecules of the tumor necrosis factor (TNF) receptor (TNFR)—associated factor (TRAF) family, most frequently TRAF2 or TRAF6 (Fig. 1). These TRAFs, through their intrinsic E3 ubiquitin ligase activity, create a platform for the activation of the tripartite inhibitor of κ B (I κ B) kinase (IKK) complex, which is composed of the kinases IKK α and IKK β and the regulatory subunit NF- κ B essential modulator (NEMO, also known as

¹Institut für Klinische und Molekulare Virologie, Friedrich-Alexander-Universität Erlangen-Nürnberg, D-91054 Erlangen, Germany. ²Abteilung Genvektoren, Helmholtz Zentrum München-Deutsches Forschungszentrum für Gesundheit und Umwelt, D-81377 München, Germany. ³Instituttfür Biochemie, Friedrich-Alexander-Universität Erlangen-Nürnberg, D-91054 Erlangen, Germany. ^{*}Present address: St. Giles Laboratory of Human Genetics of Infectious Diseases, The Rockefeller University, New York, NY 10065, USA. †Corresponding author. E-mail: Brigitte.Biesinger@viro.med.uni-erlangen.de

IKKγ). Activation of this complex is the key event in canonical NF- κ B signaling, and therefore, it is common to all stimuli. The main targets of the IKK complex are I κ B molecules that sequester preformed NF- κ B dimers in the cytoplasm (Fig. 1). Upon phosphorylation-dependent proteasomal degradation of I κ B, canonical NF- κ B dimers (prototypically the p65:p50 heterodimer) are liberated to translocate to the nucleus and exert their transcriptional activity (Fig. 1) (1).

Noncanonical NF-κB responses are initiated by distinct members of the TNFR superfamily, including CD40, lymphotoxin- β receptor (LT β R), and B cell-activating factor (BAFF) receptor (BAFFR), and depend on the NF-κBinducing kinase (NIK) (Fig. 1). In unstimulated cells, basal NIK protein amounts are controlled by a degradative, Lys⁴⁸ (K48)-dependent ubiquitin ligase complex composed of TRAF3, TRAF2, and cellular inhibitor of apoptosis 1 (cIAP1), cIAP2, or both. The predominant E3 ubiquitin ligases within this complex, cIAP1 and cIAP2, are recruited by a direct interaction with TRAF2. TRAF3, through distinct binding sites, serves as a bridging factor between TRAF2 and NIK. Whether basal NIK turnover requires the E3 ligase activities of TRAF3 and TRAF2 has not been analyzed in depth (7, 8). Upon receptor ligation, the degradative complex relocalizes from the cytoplasm, the site of NIK interaction, to occupied receptors and becomes spatially separated from NIK. This displacement is complemented by destabilization of the TRAF-cIAP complex. As originally described for CD40 ligation, destabilization is achieved by a TRAF2-dependent redirection of cIAP activity, which leads to the degradation of TRAF3 and TRAF2 (Fig. 1) (7, 8). Alternative destabilizing mechanisms, however, may apply for other receptors (9, 10). Eventually, all of these processes enable the accumulation of NIK. Subsequently, NIK induces activation of IKKα homodimers, which then phosphorylate the NF-kB subunit p100. This phosphorylation marks an IkB-like part of p100 for proteasomal degradation. The residual active moiety p52, together with its binding partner RelB, eventually translocates into the nucleus to exert transcriptional activity (Fig. 1) (11–13).

Together, receptor-proximal signaling events in canonical and noncanonical NF-κB pathways are largely controlled by TRAFs. TRAF6 specifically mediates canonical activation, and TRAF3 is generally assigned to the destabilization of NIK in the noncanonical pathway. However, TRAF2 has the potential to induce both signaling cascades because its recruitment to NF-κB-inducing receptors can contribute to both activation of the IKK complex and stabilization of NIK (Fig. 1) (14). The ability to distinguish between canonical and noncanonical NF-κB responses is further complicated by additional nonseparable features: TRAF2 and TRAF3 frequently share common binding sites on the surfaces of their interaction partners (15, 16); aberrant NIK accumulation activates the IKK complex and, thus, canonical NF-κB signaling (Fig. 1) (17, 18); and the noncanonical precursor molecule p100 may also serve as an IκB-like protein for canonical NF-κB dimers (Fig. 1) (19). Hence, it is still a matter of debate whether canonical and noncanonical NF-κB pathways exist as two separable entities or whether they are both embedded in a global NF-κB network that balances cellular responses in a stimulus- and time-dependent manner.

We previously showed that the Tio oncoprotein of the T-lymphotropic virus *Herpesvirus ateles* serves as a molecular probe to decipher oncogen-

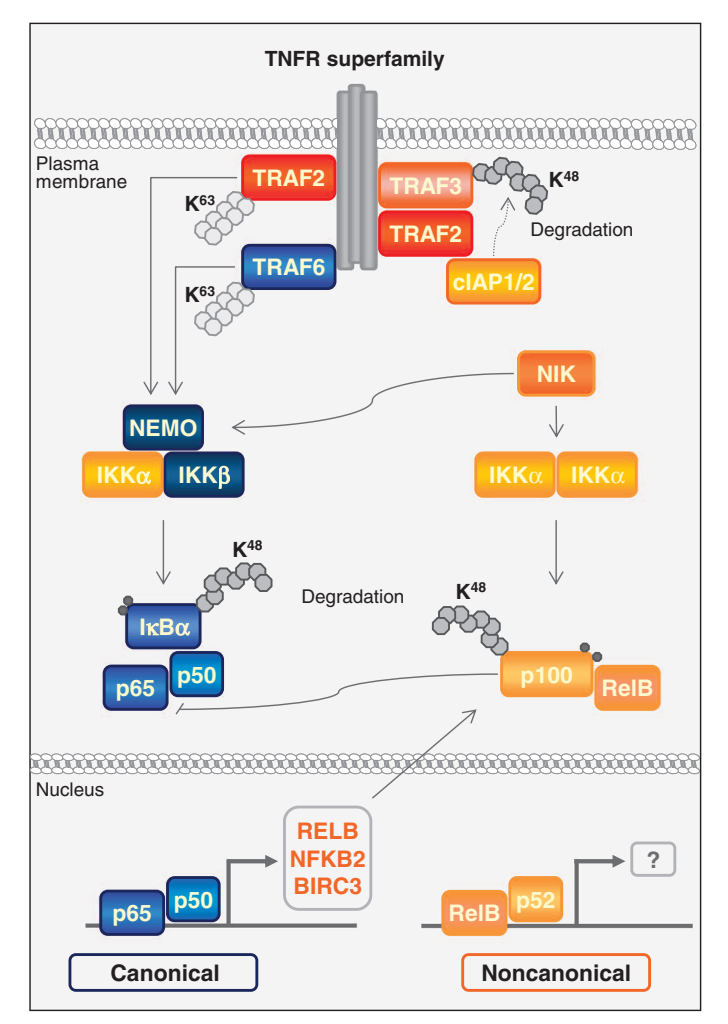


Fig. 1. Overview of NF- κ B signaling cascades and crosstalk between the two pathways. Components of canonical NF- κ B signaling are depicted in blue, whereas components of noncanonical NF- κ B signaling are shown in yellow. K⁴⁸, Lys⁴⁸-linked polyubiquitin; K⁶³, Lys⁶³-linked polyubiquitin; \bullet , phosphorylation.

ic signaling cascades in T cells. Tio is an oligomeric, membrane-bound protein that mimics a ligand-independent receptor constitutively linked to Src family kinase (SFK) and NF-κB signaling (20, 21). Activity of these pathways is essential to sustain T cell transformation by Tio-expressing herpesviruses (22–24). Tio triggers canonical NF-κB signaling through the direct recruitment of TRAF6 to its N terminus. Further downstream, Tio requires both NEMO and IKKβ activity to induce the canonical target genes encoding cIAP2, interleukin-8 (IL-8), RelB, and p100. In addition, Tio activates noncanonical NF-κB signaling, including stabilization of NIK, processing of p100 to p52, and nuclear translocation and DNA binding of the p52 and RelB subunits. This noncanonical NF-κB activation is independent of the canonical cofactors TRAF6 and NEMO and of IKKβ activity as well as the Tio-SFK interaction (24) and suggests that noncanonical NF-κB signaling is a separable entity.

To gain insight into how selectivity is achieved within the NF- κ B network, we explored the molecular mechanism of the insulated activation of noncanonical NF- κ B signaling by Tio. Our results demonstrate that Tio has a TRAF-binding motif that includes an extension not conserved in other TRAF3-binding partners. This motif directly and selectively recruits TRAF3 to mediate its subcellular redistribution and subsequent noncanonical NF- κ B activation without affecting the expression of target genes of canonical NF- κ B signaling. Hence, these data suggest that the particular mode of Tio-TRAF3 interaction constitutes a distinct molecular mechanism of noncanonical NF- κ B activation.

RESULTS

Tio-induced noncanonical NF-κB activity depends on a putative TRAF3-binding motif

We previously reported a strong and selective activation of noncanonical NF-κB signaling by the herpesviral oncoprotein Tio, which is accompanied by stabilization of the effector kinase NIK (24). Here, we investigated the underlying mechanism. To identify the regions of Tio involved in noncanonical NF-kB activation, we generated a series of truncation variants of Tio (Fig. 2A). We used the processing of p100 to p52 as a readout for activation of noncanonical NF-κB signaling. As previously reported, Tio induced p100 processing independently of the regions containing its phosphorylation site at ${\rm Tyr}^{136}~({\rm Y}^{136})$ and the known binding sites for TRAF6 (T6b) and SFKs (SH3b), whereas the increased p100 abundance was restricted to wild-type Tio and Tio mutants containing an intact T6b motif (Fig. 2B and fig. S1). Our deletional analysis showed that the induction of p100 processing required a membrane-proximal region of Tio, spanning amino acid residues 207 to 222 (Fig. 2B and fig. S1). Similar results were obtained in experiments with a NEMO-deficient Jurkat cell line in which induction of the gene encoding p100 was absent because of the lack of canonical NF-kB signaling (Fig. 2B and fig. S1).

To date, all receptors and viral mimics that stimulate noncanonical NF-κB signaling recruit TRAF3, TRAF2, or both to deplete the cytoplasmic pools of these inhibitors of NIK stability (11, 12, 16). Therefore, it was tempting to speculate that Tio used a similar mechanism to enable the accumulation of NIK, as previously observed (24). Consistent with this hypothesis, we found that amino acids 207 to 222 are located next to a potential TRAF-binding core motif ²²²SQQATD²²⁷ in Tio (Fig. 3A). This motif is reminiscent of the TRAF2- and TRAF3-binding site ²⁰⁴PQQATD²⁰⁹ described for the Epstein-Barr virus oncoprotein latent membrane protein 1 (LMP1) (13), which is related to Tio (Fig. 3A). To further investigate the structural basis for noncanonical NF-κB activation by Tio, we performed molecular modeling of a putative Tio-TRAF3 complex on the basis of the crystal structure of the LMP1-TRAF3 complex (25). The calculations

included the potential core motif ²²²SQQATD²²⁷ of Tio as well as the functionally important N-terminal adjacent residues ²¹⁰PQIILREATEVE²²¹ that we identified as important for the processing of p100 in our deletional analysis experiments. Binding of the Tio core motif mapped to TRAF3 residues that are well conserved among TRAF2, TRAF3, and TRAF5 (Fig. 3, B and C). In addition, the model predicted that the flanking residues could form numerous contacts with TRAF3 (Fig. 3B). However, these interactions mainly involved residues that are not conserved in the TRAF family (Fig. 3C). Thus, the model suggested TRAF3 binding by Tio through contacts with its core motif, which are supplemented by interactions of the flanking residues 210 to 221 with a nonconserved surface patch of TRAF3.

On the basis of the structural model, we introduced a series of point mutations into the full-length Tio protein. In the mutants mT3b.1, mT3b.2, and mT3b.3, bulky or charged amino acids of the flanking region ²¹⁰PQIILREATEVE²²¹ that were predicted to make contact with nonconserved residues on TRAF3 were substituted, whereas in the mutant mT3b.4, we replaced the anchor residues of the potential core motif ²²²SQQATD²²⁷ (Fig. 4A). Subsequently, we tested all of the mutants for their ability to induce noncanonical NF-κB signaling, as measured by detection of the processing of p100 to p52. We found that the introduction of

mutations into the anchor positions of the potential TRAF-binding core motif (mutant mT3b.4) was insufficient to impair Tio-induced p100 processing (Fig. 4, B and C). Substitution of P210 and E216 (mT3b.1) in the flanking region only marginally affected p100 processing by Tio; however, multiple substitutions in the flanking region (mT3b.2 and mT3b.3) led to a marked reduction in noncanonical NF- κ B activation (Fig. 4, B and C). Consistent with the molecular model, these data suggest that Tio depends on its extended putative TRAF3-binding motif, which is not conserved in other TRAF3-binding proteins, to induce noncanonical NF- κ B activity.

Tio-induced noncanonical NF-κB activity correlates with TRAF3 binding

We tested the proposed formation of a complex consisting of Tio with TRAF3, TRAF2, and cIAP2 in coimmunoprecipitation experiments performed with three independent T cell lines that were generated from human peripheral blood lymphocytes (PBLs) by transformation with Tio-expressing viruses [1763, 1765, 1766 (23)]. Untreated Jurkat cells served as an NF-κB-independent T cell control. Precipitation of Tio from all of the PBL lines yielded complexes that contained both TRAF3 and TRAF2 but not cIAP2 (Fig. 5A). These findings were confirmed by reciprocally precipi-

tating endogenous TRAF3 and TRAF2 (Fig. 5, B and C). We observed that cIAP2 formed complexes with TRAF2, but not TRAF3, in two of the three cell lines tested (1763 and 1765; Fig. 5C). Consistent with this, precipitation of cIAP2 yielded complexed TRAF2 only from the cell lines 1763 and 1765 (Fig. 5D). The absence of cIAP2 in Tio immunoprecipitates may be explained by the fact that this ubiquitin ligase is not recruited into the Tio complex. Alternatively, the amount of precipitated cIAP2, the most distant binding partner in the complex, might be below the limit of detection. Nevertheless, Tio nucleates a complex containing TRAF3 and TRAF2, thereby sequestering these inhibitors of NIK stability and noncanonical NF-κB activity.

To test this hypothesis, we verified the absence of NIK from Tio-nucleated complexes in the virus-transformed T cell lines by reciprocal coimmunoprecipitation of Tio and NIK (fig. S2A). We detected precipitated endogenous NIK in all three cell lines (fig. S2A); however, Tio did not coimmunoprecipitate with NIK. In the reverse immunoprecipitation, precipitated Tio-containing immune complexes did not contain NIK (fig. S2A). In contrast, TRAF3 was always associated with Tio, but not with NIK (fig. S2A). These findings suggest that the NIK-TRAF3 complex is disrupted by Tio. To unequivocally rule out the presence of NIK in Tio-nucleated, TRAF-containing complexes, we overexpressed NIK, Tio, and TRAF3 in transfected Jurkat cells (fig. S2B). Immunoprecipitation of NIK from vector-transfected (control) cells coimmunoprecipitated TRAF3. This finding indirectly indicated the presence of NIK,

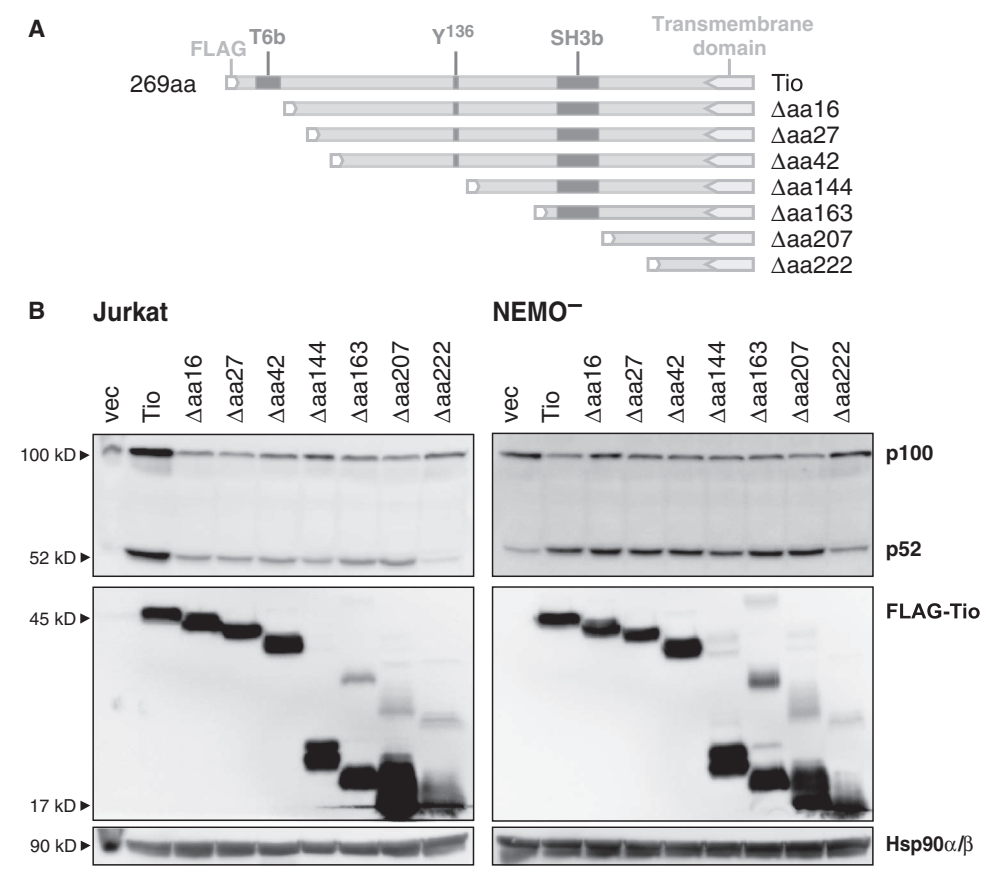


Fig. 2. Processing of p100 in the presence of Tio deletion mutants. (A) Schematic representation of Tio and its deletion mutants (Δ aa16 to Δ aa222). Known interaction motifs are indicated at the top. Y, tyrosine; aa, amino acid. (B) Jurkat cells and NEMO-deficient (NEMO⁻) Jurkat cells were transfected with plasmids encoding FLAG-tagged wild-type Tio or the indicated mutants. Western blotting analysis was performed 48 hours after transfection to detect the processing of endogenous p100 to generate p52. The presence of Tio proteins was confirmed with an antibody against FLAG, and Hsp90 α / β served as a loading control. vec, vector. Data are representative of three independent experiments. See fig. S1 for quantification of data.

Α

which itself was below the limit of detection. Upon expression of Tio, precipitated NIK was readily detectable, although TRAF3 was no longer associated with precipitated NIK. Furthermore, Tio did not coimmunoprecipitate with NIK (fig. S2B). Reciprocal Tio immunoprecipitations from the same lysates showed the Tio-TRAF3 interaction and the absence of NIK from these complexes (fig. S2B). These data suggest that Tio displaces TRAF3 from NIK to enable its accumulation.

To further assess the requirement of the identified potential TRAF3-binding motif of Tio, we performed glutathione *S*-transferase (GST) pulldown experiments with purified GST-tagged Tio (GST-Tio) and GST-mT3b.2 in combination with purified recombinant His-tagged TRAF domains. The TRAF6-binding-deficient Tio mutant GST-mT6b served as a specificity control. Precipitation of the GST-Tio fusion proteins revealed no direct interaction with recombinant TRAF2 (Fig. 6A). However, TRAF3 was readily precipitated by Tio, but not by mT3b.2 (Fig. 6A). TRAF6 was used as pulldown

control and could only be captured with Tio variants containing the T6b site (Fig. 6A). Tio thus directly interacted with TRAF3. TRAF2, which could be detected in immunoprecipitated Tio-containing complexes (Fig. 5), was not recruited directly but likely through heterodimerization with TRAF3 (12).

Next, we tested the identified motif in detail for its relevance for TRAF3 binding. To this end, we performed coimmunoprecipitation experiments with Jurkat cells coexpressing FLAG-tagged wild-type or mutant Tio as well as TRAF3. We detected the binding of TRAF3 by wild-type Tio as well as by the mutants mT3b.1 and mT3b.4 (Fig. 6B), which respectively contain two amino acid substitutions in the elongated TRAF3-binding motif or mutations in the SQQATD TRAF-binding core region. These findings are consistent with the ability of these Tio variants to induce noncanonical NF-κB signaling by means of p100 processing (Fig. 4B). Both mT3b.2 and mT3b.3 contain multiple amino acid substitutions in the extended TRAF3-binding motif, and they showed defects in

```
core
        <sup>207</sup>KNGPQIILREATEVESQQATDGQLNHRVEKVEKKLT
Tio
        <sup>146</sup>PPGEDPGTTPPGHSVPVPAT-ELGSTELVTTKTAGPE<sup>182</sup>
BAFFR
        189QRHSDEHHHDDSLPHPQQATDDSGHESDSNSNEGRH-224
LMP1
        <sup>235</sup>EINFPDDLPGSNTAAPVQET-LHGCQPVTQEDGKESR<sup>270</sup>
CD40
        °98FLVWRRCRREKFTTPIEETGGEGCPAVALIQ----
Fn14
        <sup>372</sup>GPGDLPATPEPPYPIPEEGDPGPPGLSTPHOEDG---
LTβR
Binding partner:
                                         BAFFR
TRAF1
       LRLMEEASFDGTFLWKITNVTRRCHESACGRTVSLFSPAFYTAKYGY
TRAF2
       VLEMEASTYDGVFIWKISDFARKRQEAVAGRIPAIFSPAFYTSRYGY
       FQVLETASYNGVLIWKIRDYKRRKQEAVMGKTLSLYSQPFYTGYFGY
TRAF3
       FKLLEGTCYNGKLIWKVTDYKMKKREAVDGHTVSIFSQSFYTSRCGY
TRAF5
TRAF4
       LEEL-SVGSDGVLIWKIGSYGRRLQEAKAKPNLECFSPAFYTHKYGY
       VAEIEAOOCNGIYIWKIGNFGMHLKCOEEEKPVVIHSPGFYTGKPGY
TRAF6
Binding partner: core
TRAF1
       KLCLRLYLNGDGTGK-RTHLSLFIVIMRGEYDALLPWPFRNKVTFML
       KMCLRIYLNGDGTGR-GTHLSLFFVVMKGPNDALLRWPFNOKVTLML
TRAF2
TRAF3
       KMCARVYLNGDGMGK-GTHLSLFFVIMRGEYDALLPWPFKQKVTLML
       RLCARAYLNGDGSGR-GSHLSLYFVVMRGEFDSLLQWPFRQRVTLML
TRAF5
TRAF4
       KLQVSAFLNGNGSGE-GTHLSLYIRVLPGAFDNLLEWPFARRVTFSL
TRAF6
       KLCMRLHLQLPTAQRCANYISLFVHTMQGEYDSHLPWPFQGTIRLTI
Binding partner:
                    Tio
                             core
       LDQN-----SETNV-ASGC
TRAF1
TRAF2
       LDQN-----NREHVIDAFRPDVTSSSFQRPV-----NDMNI-ASGC
       MDOGS----SRRHLGDAFKPDPNSSSFKKPT-----GEMNI-ASGC
TRAF3
TRAF5
       LDQS-----GKKNIMETFKPDPNSSSFKRPD-----GEMNI-ASGC
TRAF4
       LDQSDPGLAKPQHVTETFHPDPNWKNFQKPGTWRGSLDESSL-GFGY
       LDQSEA--PVRQNHEEIMDAKPELLAFQRPT----IPRNPKGFGY
TRAF6
```

TRAF binding

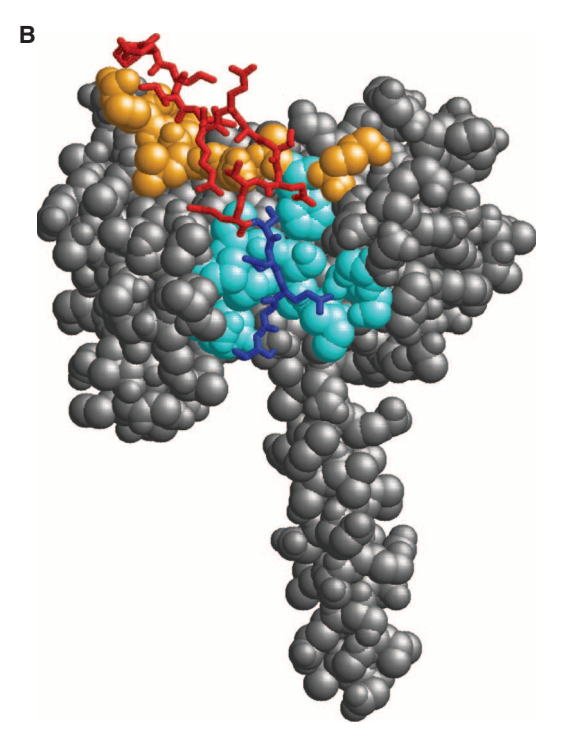


Fig. 3. Selectivity of Tio-TRAF3 interactions. (A) Multiple sequence alignments of the TRAF3-binding proteins Tio, hBAFFR, LMP1, hCD40, hFn14, and hLTβR. The consensus TRAF-binding core motif PxQxT or [PSAT]x[QE]E is highlighted in blue. Additional sequence stretches involved in the recognition of TRAF3 are marked in red for Tio and in green for BAFFR. (B) Model of the Tio-TRAF3 complex. Tio is shown in stick representation, and the core and flanking regions are colored blue and red, respectively. TRAF3 is shown in space-filled representation. Residues interacting with the core and flanking regions of Tio are colored cyan and orange, respec-

tively. (C) Multiple sequence alignments of human TRAF1 to TRAF6. TRAF residues that interact with the core binding motif of the binding partner are indicated in cyan. TRAF3 residues that make contact with the flanking residues of Tio are marked orange. TRAF residues that interact with the extended BAFFR motif are depicted in green. Gray boxes highlight the contact regions in the most similar TRAF family members, namely, TRAF2, TRAF3, and TRAF5.

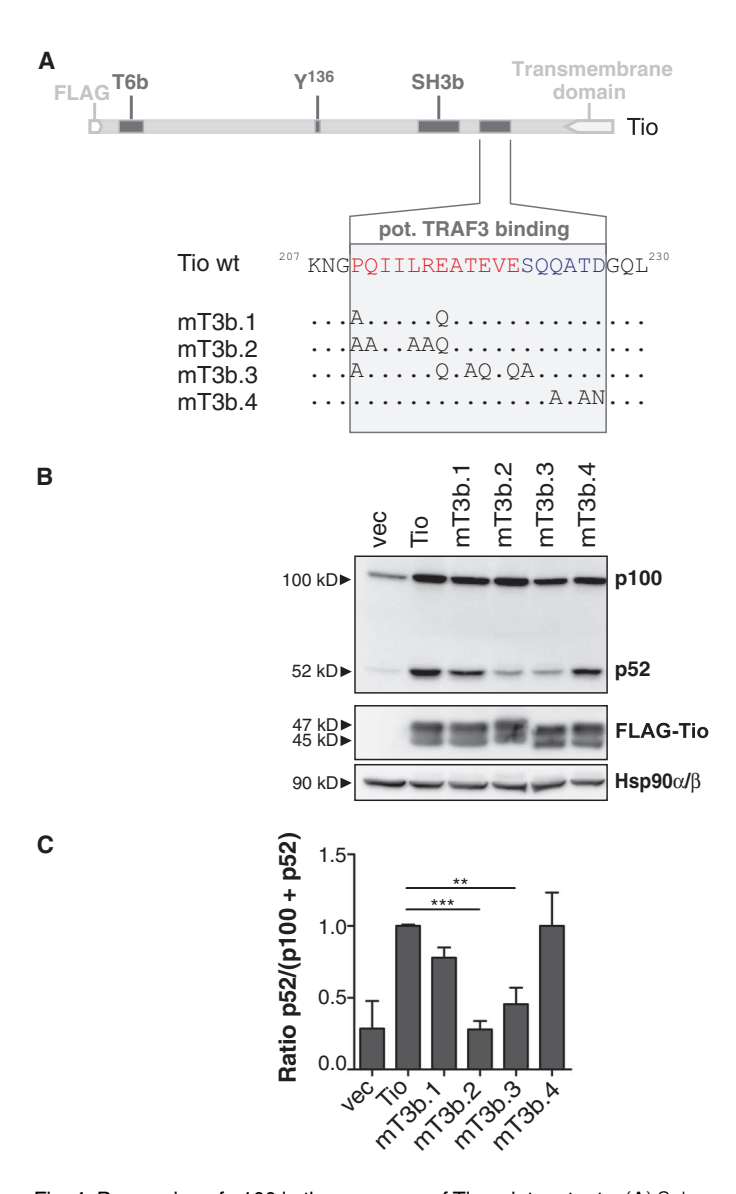


Fig. 4. Processing of p100 in the presence of Tio point mutants. (A) Schematic representation of Tio with a magnified view of the amino acid sequence from residues 207 to 230. Amino acid exchanges in the potential (pot.) TRAF3-binding motif (for mT3b.1, mT3b.2, mT3b.3, and mT3b.4) are indicated below the sequence of wild-type (wt) Tio. (B) Jurkat cells were transfected with plasmids encoding wild-type Tio or its mutants. Forty-eight hours after transfection, Western blotting analysis was performed to detect the processing of endogenous p100 to generate p52. The presence of Tio was confirmed with an antibody against FLAG, and Hsp90α/β served as a loading control. Data are representative of three independent experiments. (C) Densitometric quantification of the bands shown in (B). The extent of the processing of p100 to p52 was calculated as the ratio of the amount of p52 to the combined amounts of p100 and p52. Values were normalized to the processing rate of wild-type Tio. Data are the means and SD of three independent experiments. **P = 0.0025 for Tio versus mT3b.3 and ***P = 0.00069 for Tio versus mT3b.2 were calculated by one-way analysis of variance (ANOVA) for independent samples.

p52 generation (Fig. 4B). Accordingly, the mT3b.2 mutant showed markedly impaired recruitment of TRAF3, whereas the mT3b.3 mutant retained the ability to bind to TRAF3 (Fig. 6B). However, the mild lysis conditions used to coimmunoprecipitate exogenous TRAF3 may have enabled residual binding provided that the flanking sequences of the motif were intact. We thus identified mT3b.2 as a loss-of-function mutant and used it as such for all subsequent experiments. In conclusion, in contrast to cellular and viral TRAF3 interaction partners, the TRAF-binding core motif of Tio is not sufficient to recruit TRAF3. Rather, we suggest that Tio uses an evolutionarily nonconserved, N-terminal extended binding motif to interact with TRAF3.

The Tio-TRAF3 interaction results in a reduction in TRAF3 abundance

Recruitment of the NIK-destabilizing TRAF-cIAP complex to stimulated receptors leads to the degradation of TRAF3 and, to a lesser extent, TRAF2, which correlates with the induction of noncanonical NF- κ B signaling (7, 8). Thus, we investigated the abundances of these signaling intermediates by Western blotting analysis. In Jurkat cells transiently expressing Tio, we detected a reduction in the abundance of TRAF3 protein (Fig. 7A and fig. S3A). The abundance of TRAF2, in contrast, was unaffected in the presence of Tio (Fig. 7A). The abundance of cIAP2 protein was increased in Tio-expressing cells (Fig. 7A), which is consistent with a previous report (24). Thus, Tio seemed to induce the degradation of TRAF3 only, leaving TRAF2 abundance unaffected.

To analyze whether the reduction in TRAF3 abundance correlated with its recruitment by Tio, we transfected Jurkat cells with decreasing amounts of plasmids encoding Tio or the TRAF3-binding-deficient mutant mT3b.2. Wild-type Tio, but not the mT3b.2 mutant, reduced the abundance of TRAF3 (Fig. 7B and fig. S3B). In contrast, the abundance of RelB, which served as a control for Tio-induced canonical NF-κB signaling, was increased by both wild-type Tio and the mT3b.2 variant (Fig. 7B). This observation indicates that the reduction in TRAF3 protein abundance was a functional consequence of its recruitment by Tio and suggests that this reduction was linked to the activation of noncanonical NF-κB signaling. To verify this, we overexpressed TRAF3 in the presence and absence of Tio. The overexpression of TRAF3 substantially reduced Tio-mediated processing of p100 (Fig. 7C), implicating the Tio-TRAF3 interaction and the subsequent reduction in TRAF3 abundance in the induction of noncanonical NF-κB signaling.

The Tio-mediated reduction in TRAF3 abundance does not involve ubiquitin ligase activity

The recruitment and degradation of TRAF3 have been described for several receptors that stimulate noncanonical NF-κB signaling. According to the mechanism established for CD40, the E3 ubiquitin ligase activity of receptor-associated TRAF2 redirects the activity of cIAP1, cIAP2, or both to mark TRAF3 for proteasomal degradation (7, 8). To test for this mechanism in Tio-expressing cells, we coexpressed Tio with wild-type TRAF2 or a TRAF2 mutant that lacks ligase activity because of deletion of its RING domain. However, coexpression of neither wild-type TRAF2 nor mutant TRAF2 had an effect on the Tio-mediated reduction in TRAF3 abundance (Fig. 8A). Furthermore, we treated transiently transfected Jurkat cells with the proteasomal inhibitor MG132 or the SMAC-mimetic compound LBW242, which inhibits cIAP1 and cIAP2 activity. However, neither compound had any effect on the amounts of TRAF3 protein in the presence of Tio (Fig. 8B). We verified inhibitor efficacy by measuring an increase in total cellular ubiquitination in the presence of MG132 and a reduction in cIAP2 protein abundance in the presence of LBW242 (Fig. 8B and fig. S4A). These findings were corroborated by prolonged treatment of Tio-expressing cells with LBW242, which affected neither endogenous nor ectopic TRAF3 protein abundance (fig. S4, B and C). We further confirmed the inhibitory efficacy of LBW242 in experiments monitoring the induction of p100 processing in the absence of other noncanonical stimuli (fig. S4, B and C) and the effect of LBW242 on the survival of T cell lines transformed by Tio-expressing viruses (fig. S4D). These results exclude proteasomal and cIAP activities as factors responsible for the Tio-mediated reduction in TRAF3 abundance.

As an alternative to proteasomal degradation, cIAP-dependent lysosomal degradation of TRAF2 contributes to noncanonical NF-κB signaling downstream of the receptor Fn14 (9). Therefore, we blocked lysosomal enzymes with the cathepsin inhibitor CA-074 Me or the cysteine protease inhibitor EST. However, neither compound had any effect on the Tio-mediated reduction in TRAF3 abundance (Fig. 8B and fig. S4E), suggesting that Tio does not use lysosomal mechanisms that induce TRAF3 degradation.

To further investigate the ubiquitin-mediated destabilization of TRAF3 in the presence of Tio, we immunoprecipitated TRAF3 and performed Western blotting analysis with a ubiquitin-specific antibody. Consistent with our earlier data, Tio did not enhance the polyubiquitination of TRAF3 (Fig. 8C). Rather, Tio, which readily communoprecipitated with TRAF3,

reduced the basal ubiquitination state of TRAF3 (Fig. 8C). Finally, we investigated whether Tio formed a complex with an E3 ubiquitin ligase directed against TRAF3 in ubiquitination assays in vitro. Whereas cIAP2, a well-established E3 ubiquitin ligase for TRAF3, was effective as a positive control for the in vitro ubiquitination of TRAF3, Tio precipitates did not include any enzymatic activity to ubiquitinate purified TRAF3 (fig. S4F). In summary, our data do not support ubiquitin-mediated degradation as the mechanism by which TRAF3 abundance is reduced in the presence of Tio.

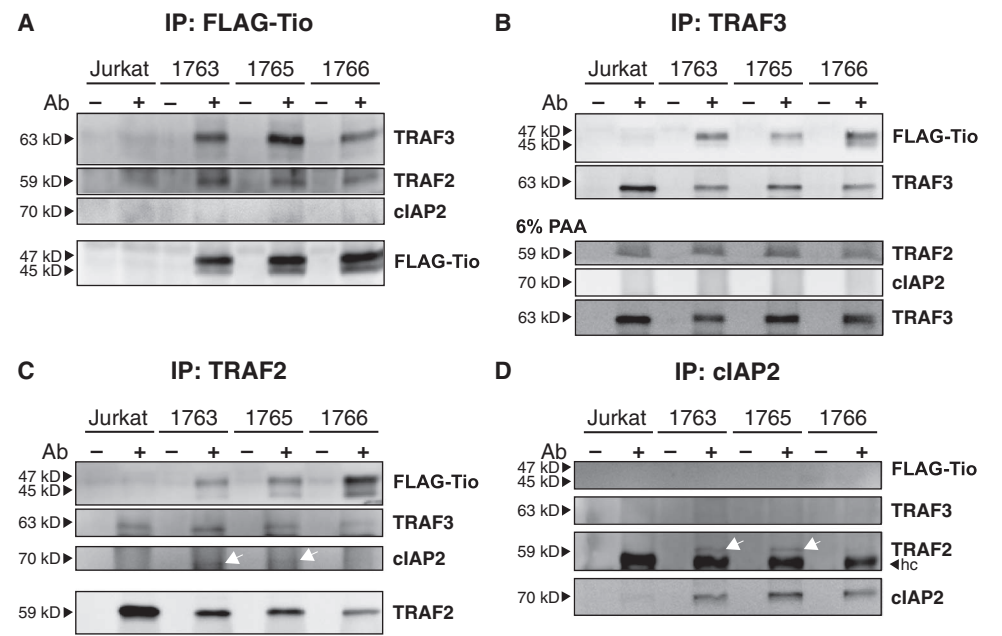
The Tio-mediated reduction in TRAF3 abundance is accompanied by redistribution of TRAF3 to insoluble cellular fractions

Given its ubiquitination-independent nature, we tested whether the reduction in TRAF3 abundance in the presence of Tio resulted from transcriptional regulation or altered protein stability. However, quantitative reverse transcription polymerase chain reaction (qRT-PCR) analysis did not reveal a reduction in the abundance of *TRAF3* transcripts in Tio-expressing cells (Fig. 8D). Similarly, the stability of soluble ectopically expressed TRAF3 protein was not altered by Tio (Fig. 8E), arguing against the increased turnover of TRAF3 protein in the solubilized cellular compartments.

Recently, BAFFR was reported to use a nondegradative mechanism to inhibit TRAF3, which is based on the redistribution of TRAF3 to an SDS-soluble cellular compartment (10). Thus, we performed differential detergent fractionation of Tio-expressing Jurkat cells. In vector-transfected control cells, TRAF3 was distributed in the cytosolic and membranous compartments (Fig. 8F). However, the expression of Tio led to a depletion of cytosolic TRAF3 and to its enrichment in an insoluble fraction that was characterized by the presence of cytoskeletal proteins such as vimentin (Fig. 8F). We did not observe this effect in cells expressing the Tio mutant mT3b.2 (Fig. 8F), suggesting that the redistribution of TRAF3 was a consequence of the Tio-TRAF3 interaction.

The Tio-TRAF3 interaction induces noncanonical NF-κB signaling without crosstalk with the canonical NF-κB pathway

Having identified TRAF3 recruitment as being responsible for the induction of noncanonical NF-κB signaling by Tio, we asked whether this interaction was also required for canonical NF-κB signaling. To this end, we tested combinatorial mutations in the TRAF3-binding motif (mT3b.2) with those in the TRAF6-binding (mT6b) and SH3-binding (mSH3b) sites for their effect on canonical and noncanonical NF-kB signaling. We observed increased amounts of p52 generation only with mutants that contained an intact TRAF3-binding motif (Fig. 9A and fig. S5). We confirmed these findings in NEMO-deficient T cells (Fig. 9A and fig. S5). Conversely, we observed an



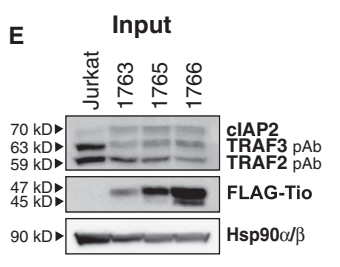


Fig. 5. Tio forms complexes with TRAF3 and TRAF2 in virus-transformed human T cells. (A to E) Virus-transformed human PBLs (lines 1763, 1755, and 1766) were subjected to immuno-precipitation (IP) with antibodies (Abs) against the targets indicated on the top of each panel (+ Ab) or without antibodies (- Ab) as specificity controls. Untreated Jurkat cells served as control. Immunoprecipitations were performed with specific antibodies against (A) FLAG-Tio, (B) TRAF3, (C) TRAF2, and (D) cIAP2. In each case, coimmunoprecipitated proteins were de-

tected by Western blotting analysis with specific antibodies, and the presence of the specific immunoprecipitated targets was verified by reincubating the membrane with the appropriate specific antibody. White arrows indicate the positions of specific proteins. (E) The presence of the immunoprecipitated proteins (cIAP2, TRAF3, TRAF2, and FLAG-Tio) in an input sample taken before immunoprecipitation was verified by Western blotting analysis. Hsp90α/β served as a loading control. hc, heavy chain; PAA, polyacrylamide. Data in all panels are representative of four independent experiments.

increase in the abundance of the canonical NF-κB target RelB only with Tio mutants containing an intact TRAF6-binding motif, whereas mutation of the TRAF3- and SH3-binding motifs did not affect the abundance of RelB (Fig. 9A). Consequently, Tio did not affect RelB abundance in the absence of NEMO (Fig. 9A).

Finally, we examined the phosphorylation of $I\kappa B\alpha$, the hallmark of canonical NF- κB induction, in cells expressing wild-type Tio or its mutants. We detected phosphorylated $I\kappa B\alpha$ only in cells in which the Tio proteins contained a TRAF6-binding site, whereas destruction of the TRAF3-binding motif did not impair $I\kappa B\alpha$ phosphorylation (Fig. 9B). The same held true for the generation of cIAP2, whose gene is a target of canonical NF- κB signaling (Fig. 9B). Thus, Tio-mediated induction of canonical NF- κB activity depended on the presence of the N-terminal TRAF6-binding site and was completely independent of the C-terminal TRAF3-binding motif. Furthermore, noncanonical NF- κB activation and the processing of p100 to generate p52 depended solely on the presence of an intact TRAF3-binding motif and were independent of Tio-TRAF6 interactions and of the presence of NEMO. In conclusion, Tio stimulated either arm of NF- κB signaling individually through a distinct protein-protein interaction motif.

DISCUSSION

We previously showed that the oncoprotein Tio induces noncanonical NF- κ B signaling by stabilization of the noncanonical NF- κ B effector kinase NIK, together with activation of the p52 and RelB subunits (24). Here, we attempted to unravel the selectivity of this response to gain insight into general mechanisms of noncanonical NF- κ B activation within the cellular NF- κ B signaling network.

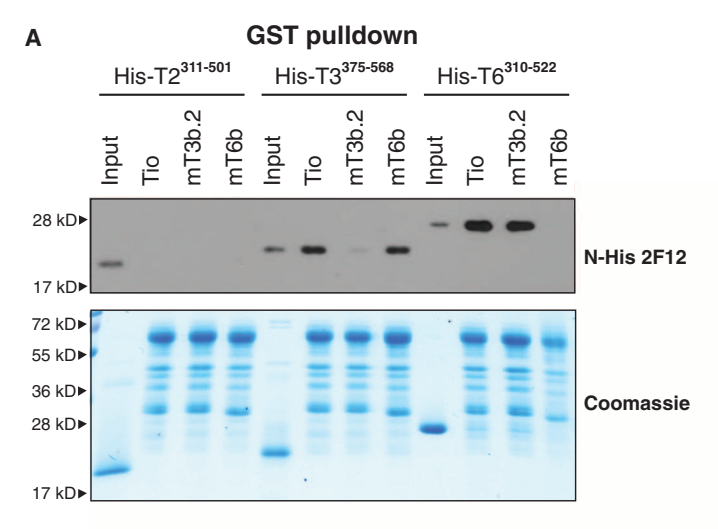
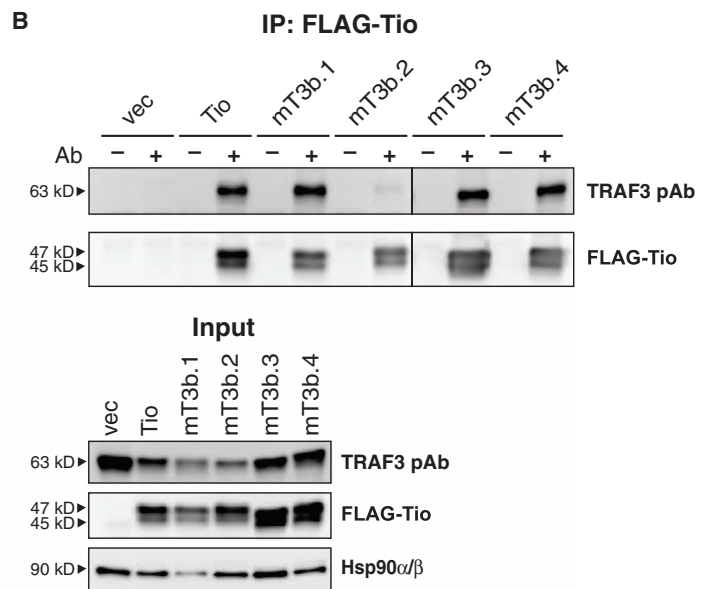


Fig. 6. Tio interacts with TRAF3, but not TRAF2, through the T3b motif. (A) Glutathione Sepharose loaded with GST fusion proteins of wild-type and mutant Tio (Tio, mT3b.2, and mT6b) was incubated with His-tagged TRAF2^{311–501} or TRAF3^{375–568} or with TRAF6^{310–522} as a control. Western blotting analysis was performed with an N-His–specific antibody to detect TRAF proteins that were pulled down. Equal protein amounts were verified with a Coomassie control gel. Twenty-five nanograms of purified TRAF protein was used as an input control for Western blots, whereas 1 μg was used for the Coomassie gels. (B) Jurkat cells were cotransfected with plasmids encoding wild-type Tio or its mutants (mT3b.1, mT3b.2, mT3b.3, or mT3b.4) and with plasmid encoding HA-TRAF3. Forty-eight hours after transfection, samples were subjected to immunoprecipitation

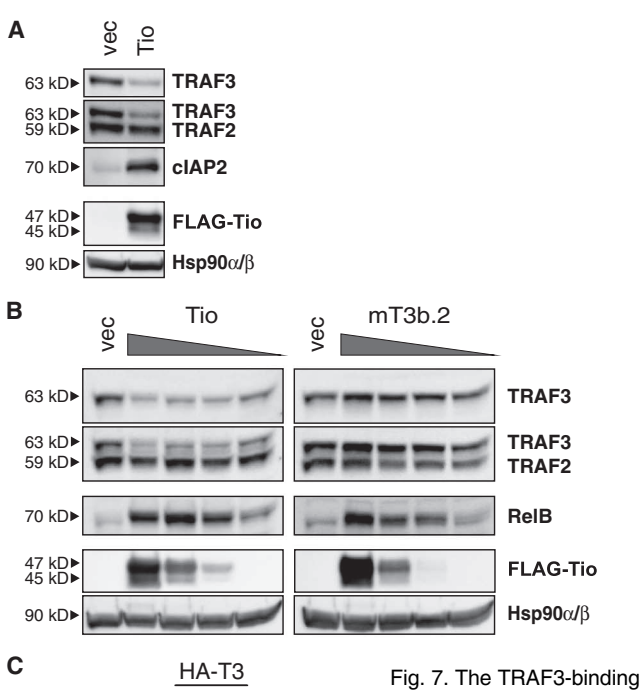
We found that the stimulation of noncanonical NF-κB signaling by Tio could be assigned to the presence of a direct TRAF3-binding site. Identification of this site enabled us to delineate the Tio-induced canonical and noncanonical NF-κB responses. Our findings demonstrate that the stimulation of canonical NF-κB signaling, including IκBα phosphorylation and canonical target gene regulation (for example, the generation of cIAP2, RelB, and p100), was completely independent of Tio-TRAF3-induced, noncanonical NF-κB signaling. Conversely, the ability of Tio to stimulate the processing of p100 and the relocalization of TRAF3, both readouts of noncanonical NF-κB activation, completely depended on the integrity of the TRAF3-interacting site of Tio and was not affected by ablation of canonical NF-kB signaling through the Tio-TRAF6-NEMO complex. Furthermore, the independence of TRAF6-NEMO-induced NF-κB signaling was previously reported for Tio-mediated NIK stabilization (24). These findings argue in favor of the two NF-kB pathways coexisting as separable entities and further establish Tio mutants as selective regulators of canonical versus noncanonical NF-κB responses. Thus, we suggest that Tio is distinct from other viral and cellular NF-kB inducers, for which extensive crosstalk has been described to interconnect canonical and noncanonical signals within the NF- κ B network (3, 26).

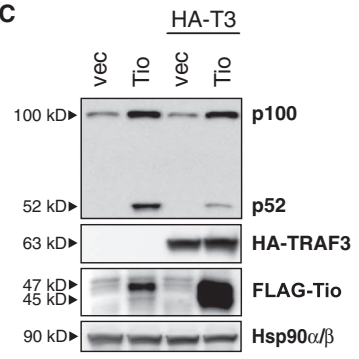
Crosstalk occurs at different levels in cytoplasmic NF- κ B signaling cascades and hampers analysis of the biological and pathological effects of the individual pathways. A well-established crosstalk mechanism originates from the production of p100 protein in response to activation of the canonical NF- κ B pathway (Fig. 1). In the absence of noncanonical stimulation (for example, upon treatment with TNF- α), the increase in p100 abundance generates a negative feedback loop because unprocessed p100 exerts an I κ B-like inhibitory function on noncanonical NF- κ B



with a FLAG-specific antibody (+ Ab). Samples treated without antibodies (– Ab) served as specificity controls. Western blotting analysis was performed to detect coimmunoprecipitated TRAF3. The immunoprecipitation of FLAG-Tio was confirmed by reincubation with a FLAG-specific monoclonal antibody (mAb). The presence of the coimmunoprecipitated proteins (TRAF3 and FLAG-Tio) was verified by Western blotting analysis of an input sample taken before immunoprecipitation (lower panel). Hsp90 α/β served as a loading control. Data in all panels are representative of three independent experiments.

signaling by sequestering RelB and on canonical NF- κ B by sequestering p65 (19, 27, 28). Upon NIK activation, the increased pool of p100 enhances noncanonical NF- κ B signaling by supplying more precursor molecules for the generation of p52 and by releasing sequestered RelB (Fig. 1) (29). Because wild-type Tio activates both NF- κ B pathways simultaneously, the increased amounts of p100 and RelB likely serve as enhancers of noncanonical NF- κ B signaling. Nevertheless, the Tio mutant mT6b, which is





rig. 7. The TRAF3-binding motif of Tio induces a reduction in TRAF3 abundance to mediate processing of p100. (A) Jurkat cells were transfected with plasmid encoding FLAG-Tio or with empty vector as a control and then were subjected to Western blotting analysis 48 hours after transfection. Endogenous TRAF3, TRAF2, and cIAP2 proteins were detected with

specific antisera. The presence of Tio was confirmed with a FLAG-specific antibody, and Hsp90 α / β served as a loading control. Data are representative of four independent experiments. (B) Jurkat cells were transfected with 50, 10, 5, or 1 μ g of plasmids encoding Tio or mT3b.2. Forty-eight hours after transfection, Western blotting analysis was performed to detect endogenous TRAF3. Blots were then reincubated with antibodies specific for TRAF2 and RelB proteins. The presence of Tio was confirmed with an anti-FLAG antibody, and Hsp90 α / β served as a loading control. (C) Jurkat cells were cotransfected with plasmids encoding Tio and HA-TRAF3. Forty-eight hours later, cells were subjected to Western blotting analysis with a specific antibody to detect the processing of p100 to generate p52. The presence of Tio and TRAF3 was confirmed with FLAG- and HA-specific antibodies, respectively. Hsp90 α / β served as a loading control. Data in (B) and (C) are representative of three independent experiments. See fig. S3 for quantification of data.

unable to induce this enhancing effect through the canonical route, still triggers p52 generation and the activation of both p52 and RelB (24). Conversely, the Tio mutant mT3b.2, which increases the abundance, but not the processing, of p100, did not impair canonical NF- κ B activity relative to wild-type Tio. These findings suggest that Tio has evolved mechanisms to distinctly activate canonical and noncanonical NF- κ B in a manner that is less prone to reciprocal interference.

Another example of crosstalk is based on the kinase-substrate relationship of NIK, which is not exclusive for IKK α homodimers in non-canonical NF- κ B signaling (Fig. 1). Rather, aberrant accumulation of NIK may activate the IKK complex and thereby promote the canonical NF- κ B axis (Fig. 1) (17, 18). Indeed, aberrant increases in NIK abundance contribute to the activation of both pathways in multiple myeloma and diffuse large B cell lymphoma (30, 31). However, we found that the accumulation of NIK in Tio-expressing cells did not result in the phosphorylation of I κ B α , the major substrate of the IKK complex, and likewise, induction of the canonical targets cIAP2 and RelB was not linked to NIK stabilization.

Further upstream, complexity is added to the NF-kB network by the fact that different TRAF molecules, which constitute the link between receptor ligation and NF-kB activation, share common binding sites. Although TRAF3 may serve as an exclusive mediator of noncanonical NF-κB signaling, its association with ligated receptors occurs through motifs that can also recruit TRAF2 and TRAF5, known linkers to canonical NF- κ B signaling (14, 26). Thus, TRAF molecules of distinct function use mutual interfaces on the cytoplasmic tails of members of the TNFR superfamily (11). Such overlapping binding sites account for the simultaneous induction of canonical and noncanonical NF-κB responses downstream of, for example, CD40 and LTβR (Fig. 1) and per se restrict selective analyses of receptor-mediated effects on either pathway, whether physiologic or pathologic (12). The data provided by our study show that Tio, like members of the TNFR superfamily, nucleates a complex containing both TRAF3 and TRAF2. However, we established direct interactions only between Tio and TRAF3.

We attribute the specificity of noncanonical NF-κB activation by Tio to its selective mode of interaction with TRAF3. This selectivity is particularly remarkable because other TRAF3-binding partners also interact with the closely related TRAFs TRAF2 and TRAF5, including LTβR (32) and LMP1 (33). This observation can be explained by the fact that the residues recognized by their core interaction motifs (PxQxT or [PSAT] x[QE]E) (34) are conserved among these three TRAF-binding factors (Fig. 3C). This makes it difficult to modulate TRAF binding specificity by sequence variations in the core motif itself. To ensure specific recognition of TRAF3, the BAFFR-TRAF3 complex [Protein Data Bank (PDB) code: 2GWK] (35) therefore relies on the extensive formation of contacts between flanking residues of the BAFFR core motif (Fig. 3A) and a surface patch of TRAF3 that is not conserved in other TRAFs (Fig. 3C). Our mutational data (Fig. 4) and the molecular model (Fig. 3) suggest that Tio also uses flanking residues to enhance its TRAF3 binding specificity. In contrast to the BAFFR-TRAF3 interaction, the flanking residues are located N-terminally adjacent to the core motif in Tio (Fig. 3A), and they make contact with a different nonconserved surface patch in TRAF3 (Fig. 3C).

In addition to the exploitation of flanking sequence stretches to enhance binding specificity, Tio and BAFFR share another interesting feature: Both exhibit mutations of key residues in the PxQxT core motif (P→S in Tio, Q→P in BAFFR; Fig. 3A) that are expected to decrease binding affinity. One explanation for this observation might be that a high-affinity core motif would mediate a tight, but nonspecific, binding to several closely related members of the TRAF family (such as TRAF2, TRAF3, and TRAF5). In such a situation, it would no longer be possible

to modulate binding specificity by additional contacts of the flanking residues because the interaction of the core motif alone would be sufficiently strong to ensure binding even in the absence of the contacts of flanking residues. On the contrary, the low-affinity core motif of Tio requires the flanking residues to increase binding affinity, and because of the specific contacts of the flanking residues, tight binding is only observed for TRAF3. This model is consistent with the results of our mutational studies (Figs. 4 and 6), suggesting that mutation of key residues in the core motif is not sufficient to disrupt binding, whereas the flanking residues are highly relevant for the interaction (mutant mT3b.2). Hence, the viral protein Tio evolved a distinct TRAF3-interacting sequence to exert BAFFR-related functions.

Finally, TRAF molecules serve as versatile rheostats in both NF- κ B pathways. In addition to its contribution to NIK destabilization, TRAF2 stimulates canonical NF- κ B signaling downstream of certain TNFR superfamily members (14, 26). This dual role of TRAF2 requires its presence for canonical and its absence for noncanonical activation of NF- κ B. Consequently,

receptors that induce NIK stabilization concomitantly lead to TRAF2 degradation. This reduction in TRAF2 abundance not only enables the accumulation of NIK but also prevents simultaneous activation of the IKK complex (36). In contrast, several lines of evidence suggest that TRAF2 is not required for Tio-induced noncanonical NF-κB activity. Tio did not directly recruit TRAF2 (Fig. 6A), affect TRAF2 abundance (Fig. 7, A and B), or depend on TRAF2 to reduce TRAF3 abundance (Fig. 8A). Hence, Tio likely evolved a TRAF2-independent mechanism of noncanonical NF-κB activation, similar to BAFFR (10). Thereby, TRAF2 is preserved for potential functions in other signaling pathways.

TRAF3 is the substrate-binding component of the TRAF-cIAP E3 ubiquitin ligase complex that controls NIK degradation in unstimulated cells. Receptor-mediated sequestration of this complex liberates NIK and terminates its degradation. Different receptors use a range of molecular strategies to further destabilize the TRAF-cIAP complex (11, 37). Although proteasomal degradation of both TRAF3 and TRAF2 has been described

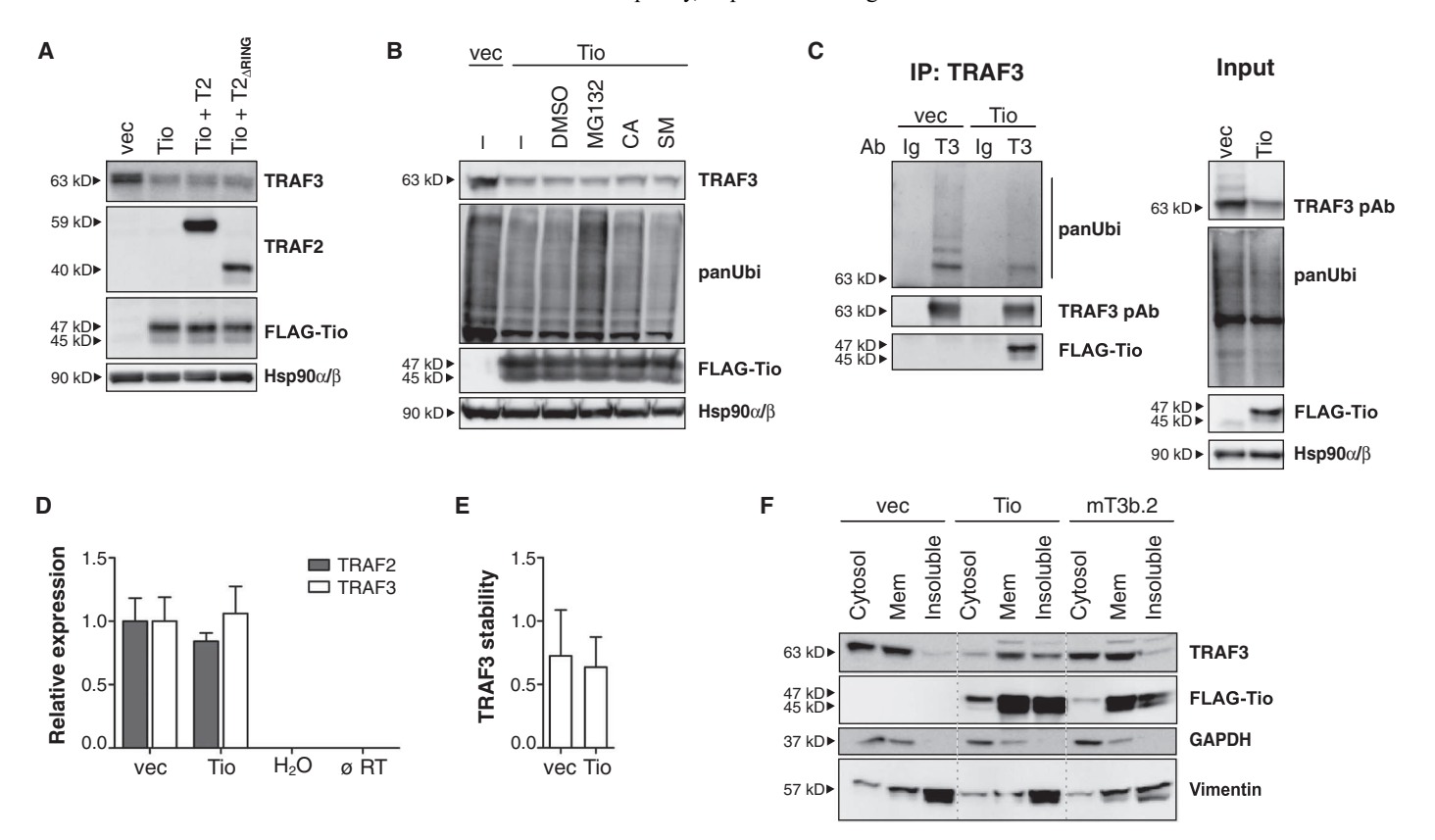
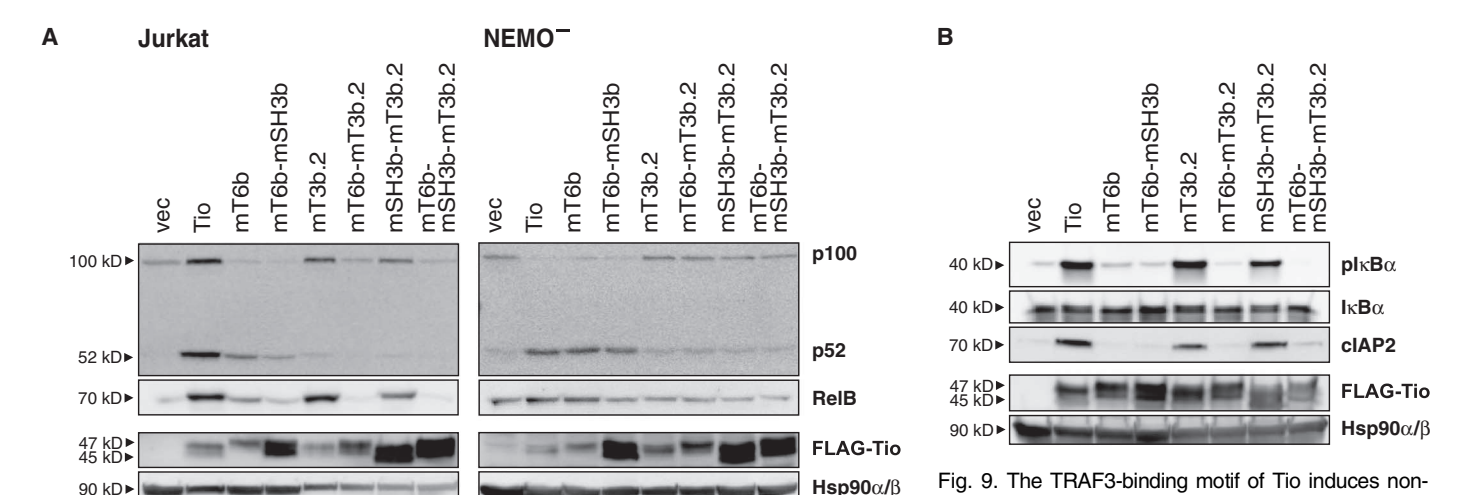


Fig. 8. Tio induces a ubiquitination-independent reduction in TRAF3 abundance through its subcellular redistribution. Jurkat cells were harvested 48 hours after transfection with plasmid encoding FLAG-Tio or with empty vector (vec) as a control. (A to C) Western blotting analysis to detect endogenous TRAF3, Tio, and Hsp90α/β. Data are representative of three independent experiments. (A) Coexpression of wild-type TRAF2 and a mutant TRAF2 lacking the RING domain (TRAF2 $_{\Delta RING}$) was confirmed by Western blotting analysis. (B) Cells were treated with MG132 for 12 hours or with CA-074 Me (CA), LBW242 (SM), or dimethyl sulfoxide (DMSO) for 24 hours before they were lysed. Cellular ubiquitination (panUbi) was detected to verify MG132 efficacy. For additional controls, see fig. S4A. (C) Ubiquitination of immunoprecipitated TRAF3 (T3) and coimmunoprecipitation of Tio were analyzed by Western blotting with antibodies against ubiquitin

(panUbi) and the FLAG tag, respectively. Input samples taken before immunoprecipitation served as controls. (D) The relative abundances of TRAF2 and TRAF3 mRNAs were determined with SYBR Green-based qRT-PCR analysis. $\rm H_2O$ and ø RT indicate negative controls. Data are means and SEM of five independent experiments. (E) Relative stability of 35 S-labeled HA-TRAF3 8 hours after removal of the labeling medium. Data are means and SD of four independent experiments. (F) Differential detergent fractionation to separate cytosolic, membrane (Mem), and insoluble cytoskeletal subcellular compartments. The distribution of endogenous TRAF3 and FLAG-Tio was determined. GAPDH (glyceraldehyde-3-phosphate dehydrogenase) and vimentin served as markers for the cytosol and cytoskeleton, respectively. Data are representative of three independent experiments.



NF-κB targets. (A and B) Jurkat cells or NEMO-deficient (NEMO⁻) Jurkat cells were transfected with plasmids encoding wild-type Tio or Tio mutants carrying individual or combined mutations in the TRAF6-binding site (mT6b), the SH3-binding motif (mSH3b), and the TRAF3-binding site (mT3b.2). Forty-eight hours after transfection, Western blotting analysis was performed to detect the processing of p100 to p52. The presence of the Tio proteins was confirmed with an anti-FLAG antibody, and Hsp90α/β served as a loading control. (A) Detection of endogenous p100, p52, and RelB. (B) Phosphorylation and abundance of endogenous IκBα and cIAP2 proteins. Data in all panels are representative of three independent experiments. See fig. S5 for quantification of data.

for CD40 and LTβR, a clear assignment of cIAP1 and cIAP2 as the ubiquitin ligases that mediate this phenomenon has been reported only for CD40 (7, 8, 38). In contrast, a lysosomal degradation mechanism regulates the stability of a TRAF2-cIAP complex involved in noncanonical NF-κB activation downstream of TWEAK-Fn14 interactions (9). Furthermore, the nondegradative sequestration of TRAF3 has been reported for ligation of BAFFR to enable p100 processing (10). However, in the case of Tio, we did not observe a requirement for cIAP activity or the degradation of TRAF3. Rather, TRAF3 was separated from NIK and depleted from the cytosolic compartment (fig. S2 and Fig. 8F). Whereas stimulation of BAFFR results in the relocation of TRAF3 to the membrane fraction (10), we found that Tio resulted in the movement of TRAF3 to a poorly soluble fraction enriched for cytoskeletal proteins. Future analyses will be needed to unravel the mechanism(s) by which TRAF3 is redistributed by Tio and BAFFR.

In summary, the viral oncoprotein Tio displays a selective mode of interacting with TRAF3 to activate the noncanonical NF-κB pathway. We conclude that Tio thereby constitutes a promising tool to study the effects of sustained noncanonical NF-κB activity. In particular, identification of noncanonical target genes may advance our understanding of lymphoid malignancies associated with excessive activation of this pathway.

MATERIALS AND METHODS

Cell culture and electroporation

The transformed PBL cell lines 1763 YYYY, 1765 YYYY, and 1766 YYYY and Jurkat cells were cultured and transfected as previously described (23, 24). Cells were harvested 48 hours after transfection and were processed for immunoprecipitation and Western blotting analysis.

Expression plasmids and reagents

To generate the pEF1-Tio expression plasmids, an Nhe I restriction site was inserted into pEF1-Tio (24) by PCR amplification to generate

pEF1-FLAG-Nhe I-Tio. Complementary DNA (cDNA) encoding truncated Tio fragments were amplified by PCR, purified, and ligated into the newly generated pEF1-FLAG-Nhe I vector at the Nhe I and Eco RI restriction sites to generate Tio deletion mutants. The pEF1-mT3b mutants (mT3b.1, mT3b.2, mT3b.3, and mT3b.4) were generated by introducing point mutations (see Fig. 4) with the QuikChange XL site-directed mutagenesis kit (Stratagene) or overlap extension PCR. The pGEX2T-Tio expression plasmids (pGEX2T-Tio, pGEX2T-mT6b, and pGEX2T-mT3b.2) had the sequences encoding the Tio transmembrane domain deleted during PCR to increase the solubility of the GST fusion proteins. The respective expression cassette was amplified by PCR from a pEF1 background and ligated into pGEX-2T (GE Healthcare) at the Bam HI and Eco RI restrictions sites. The plasmids pEF1-HA (hemagglutinin)-TRAF3, pEF1-NIK, and pEF1-HA-ubiquitin were generated by PCR amplification of the respective cDNA cassettes and ligation into pEF1 at the Bam HI and Eco RI, Bam HI and Sac I, or Bam HI and Xba I restriction sites, respectively. Primer sequences are listed in table S1. The integrity of all expression cassettes was verified by DNA sequencing on an ABI 3130XL. The plasmids pRK5-TRAF2 und pRK5-TRAF2^{87–501} (TRAF2_{ARING}) were described previously (39). The SMAC-mimetic compound LBW242 was a gift of Novartis Pharma AG. Transfected Jurkat cells were treated with 10 μ M LBW242 for 24 or 40 hours before harvesting. Virus-transformed human T cell lines (1763, 1765, and 1766) were treated with the same concentrations of reagents for 9 days, and cells were split and inhibitor was replenished every 48 hours. The proteasome inhibitor MG132 (0.1 μM; Cayman Chemical), the cysteine protease inhibitor EST (10 μM; Calbiochem), and the cathepsin B inhibitor CA-074 Me (4 µM; Calbiochem) were applied to Tio-expressing Jurkat cells and vector-transfected controls for 12 (MG132) or 24 hours, respectively, before cells were harvested.

canonical NF-κB signaling without affecting canonical

RNA isolation, cDNA synthesis, and qRT-PCR

RNA isolation and cDNA synthesis were performed as described previously (40). qRT-PCR was performed in duplicate samples with SYBR Green dye (Invitrogen) on an Applied Biosystems 7500 detection system. A 25-µl reaction contained 0.12 µM carboxy-X-rhodamine (ROX) (Invitrogen),

3.5 mM MgCl₂, 0.8 mM dNTPs (deoxynucleotide triphosphates), 0.1× SYBR Green, 0.1 pmol of each primer, 1.25 U of Crimson Taq DNA Polymerase (New England Biolabs), and 1 μ l of the cDNA reaction. Cycling conditions were 95°C for 10 min, 40 cycles of 95°C for 15 s and 60°C for 1 min, followed by a dissociation stage of 95°C for 15 s, 60°C for 1 min, and 95°C for 15 s. Primer sequences are listed in table S1. The abundances of *TRAF2* and *TRAF3* mRNAs were quantified relative to that of *HPRT1* mRNA with the $\Delta C_{\rm T}$ method, and vector controls were set to 1 for normalization. Depicted in the appropriate figures are the means and SEM of five independent experiments.

Immunoprecipitations

Jurkat cells (10×10^6) and virus-transformed PBL cell lines (50×10^6 cells) were lysed in 500 µl or 1 ml of TNE lysis buffer, respectively (supplemented with the inhibitors aprotinin, NaF, N-ethylmaleimide, Na₃VO₄, leupeptin, and MG132), with 0.5% NP-40 as a detergent. Two percent of the lysate was taken aside as the input control. To detect polyubiquitinated proteins, we resuspended Jurkat cells (8×10^6) in 100 µl of radioimmunoprecipitation assay (RIPA) buffer (supplemented with inhibitors), immediately mixed with the same volume of 2% SDS in tris-buffered saline, and boiled at 95°C until clear (~20 min). For all lysis conditions, cleared lysates were incubated with 2 to 4 µg of the indicated antibodies [against Tio (20) (figs. S2B and S4F) or the FLAG epitope (M2), TRAF3, TRAF2, cIAP2, NIK, HA, or an immunoglobulin (Ig) control] at 4°C on an overhead tumbler for 2 to 16 hours. Protein A-coupled magnetic Dynabeads (50 µl from stock solution; Invitrogen) were added, and antibody-bound protein was captured from the lysate for 1 hour at 4°C on an overhead tumbler. Beads were washed three times with 200 μ l of lysis buffer, resuspended in 100 μ l of lysis buffer, and transferred to new reaction tubes to avoid co-elution of protein unspecifically bound to the tube wall. The beads were resuspended in 25 µl of 2× Roti-Load 1 buffer (Roth) and boiled at 95°C for 5 min. All depicted data are representative of at least three independent experiments, as detailed in the figure legends.

Determination of TRAF3 stability

Jurkat cells were cotransfected with the plasmids pEF1-HA-TRAF3 and either pEF1 or pEF1-Tio. Twenty-four hours after transfection, cells were washed, resuspended in long-term labeling medium, supplemented with [35S]methionine (20 µCi/ml), and incubated for 16 hours to reach steadystate labeling (41). Cells were washed, resuspended in chase medium (41), divided into aliquots (of \sim 5 to 10×10^6 cells each), and harvested either immediately for the reference value or after 8 hours of incubation at 37°C. Cell pellets were stored at -80°C and lysed in 500 µl of RIPA buffer [10 mM tris-HCl (pH 8.0), 150 mM NaCl, 2 mM EDTA, 1% NP-40, 0.1% SDS, 0.5% sodium deoxycholate], supplemented with inhibitors as listed for immunoprecipitations. The protein concentration of each lysate was determined in duplicate with the bicinchoninic acid (BCA) assay (Uptima). Ectopic TRAF3 was immunoprecipitated with anti-HA antibodies. Precipitated proteins were resolved by 10% SDS-polyacrylamide gel electrophoresis (SDS-PAGE). Gels were fixed, dried, and exposed for 3 days to a TR2040 screen (Fuji), which was scanned with a CR 35 BIOplate reader (Dürr Medical). Band intensities were quantified with an AIDA Image Analyzer 4.22 software (raytest) and normalized for the protein content of the lysates. TRAF3 stability was calculated as the ratio of the 8-hour value relative to the reference value. Data are given as the means and SD of four independent experiments.

GST pulldowns

Glutathione Sepharose 4B beads (10 μ l; 50% slurry) (GE Healthcare) were loaded with 80 μ g of GST-Tio, GST-mT3b.2, or GST-mT6b at 4°C for 4 hours on an overhead tumbler. Beads were pelleted at 500g for 5 min

at 4°C and were washed twice with phosphate-buffered saline (PBS). After washing, the GST-Tio–loaded beads were incubated with 3 μ g of bacterially expressed and purified His-TRAF2³¹¹⁻⁵⁰¹, His-TRAF3³⁷⁵⁻⁵⁶⁸, or His-TRAF6³¹⁰⁻⁵²² in 500 μ l of PBS, 0.1% (v/v) Tween 20, 0.1% (w/v) bovine serum albumin for 1 hour at 4°C end-over-end. Beads were pelleted and washed three times with PBS, 0.1% Tween 20. Beads were then resuspended in 75 μ l of 1× SDS sample buffer and boiled at 95°C for 5 min.

Subcellular fractionation

Fractionations were performed with the subcellular protein fractionation kit (Thermo Scientific) according to the manufacturer's instruction. Depicted in the appropriate figures are fraction 1 (cytosol), fraction 2 (membranes), and fraction 5 (pellet and cytoskeleton).

Antibodies and Western blotting

Jurkat cells and transformed PBL cell lines were lysed and subjected to Western blotting analysis as described previously (21, 24). The primary antibodies used were specific for cIAP2 (58C7), IκBα (L35A5), pIκBα (5A5), NIK, and p100/p52 (18D10) (all from Cell Signaling Technology); the FLAG epitope [M2, horseradish peroxidase (HRP)-coupled or unlabeled; Sigma]; the HA epitope (HA.11-16B12; Covance); N-His (2F12) (42), RelB (C-19), Hsp90α/β (F-8), TRAF3 (H-122), TRAF3 mAb (G-6), TRAF2 (H-249), TRAF2 mAb (G-3), ubiquitin (P4D1, HRP-coupled) (all from Santa Cruz Biotechnology). Normal rabbit and mouse IgG (Santa Cruz Biotechnology) were used as immunoprecipitation controls. Secondary antibodies were HRP-coupled anti-mouse Ig F(ab), (GE Healthcare) or anti-rabbit Ig (P0399; Dako). Detection by enhanced chemiluminescence was performed with a Kodak Image Station 4000MM PRO camera. All depicted data are representative of at least three independent experiments; see the figure legends for details. Densitometric quantification of Western blots was performed with an AIDA Image Analyzer 4.22 software (raytest). The extent of processing of p100 to generate p52 was calculated by dividing the amount of p52 by the sum of the amounts of p100 and p52. Values were normalized to the processing rate of wild-type Tio. The amounts of TRAF3 were calculated as the ratio of TRAF3 and Hsp90α/β. Relative TRAF3 abundance in samples was normalized to that of vector-transfected control samples. Depicted data are presented as means and SD of three independent experiments.

Molecular modeling of the Tio-TRAF3 complex

Modeling of the Tio-TRAF complex was performed with the LMP1-TRAF3 complex crystal structure as a template (PDB code: 1ZMS) (25). Because of the short length of LMP1, the respective complex enabled the modeling of only residues 222 to 228 of Tio. Therefore, the orientation of the adjacent N-terminal residues in Tio was deduced from the complex of vIRF4 with the TRAF-like domain of the HAUSP protease (PDB code: 2XXN) (43). Modeling was performed with Modeller 9v3 (44) followed by energy minimization with Sybyl7.3 (Tripos Inc.). Analysis of the TRAF3-binding protein contacts was performed with DIMPLOT (45), and RasMol (46) was used for structure visualization. Multiple sequence alignments for TRAF3-binding proteins (Tio, hBAFFR, LMP1, hCD40, hFn14, and hLTβR) and for human TRAF factors were performed with ClustalW (47) with standard settings.

In vitro ubiquitination assays

The assay kit (SK-10) and reagents were purchased from Boston Biochem. Reactions contained recombinant, purified E1 (E-305) and E2 enzymes (K-980), as well as ubiquitin (U-100H), and the ubiquitination assays were performed according to the manufacturer's instructions with 4 µg of recombinant His-TRAF3³⁷⁵⁻⁵⁶⁸ as the substrate. Proteins with putative E3 ubiquitin ligase activities (FLAG-Tio and endogenous cIAP2) were immuno-

RESEARCH ARTICLE

precipitated and added to the reaction mixture for 90 min at 25°C. Subsequently, the bead-bound putative E3 ubiquitin ligases were recovered from the reaction and processed as described for immunoprecipitations. The reactions were stopped and mixed with an equal volume of 4× Roti-Load 1 buffer (Roth) and boiled at 95°C for 5 min.

Viability measurements

Cells were stained with propidium iodide (PI; $10\,\mu\text{g/ml}$) and subjected to flow cytometric analysis with an LSR II flow cytometer (BD Biosciences). PInegative cells were considered to be viable and are depicted as percentages of the total cell population. The means and SEM of six experiments are depicted.

Statistical analysis

Statistical computation was performed with the tools available at http://vassarstats.net/. The applied tests and the obtained *P* values are specified in the corresponding figure legends.

SUPPLEMENTARY MATERIALS

www.sciencesignaling.org/cgi/content/full/6/272/ra27/DC1

Fig. S1. Quantification of the extent of processing of p100 to p52 in the presence of Tio deletion mutants.

- Fig. S2. Tio does not form complexes with NIK.
- Fig. S3. Quantification of TRAF3 protein abundance in the presence of Tio.
- Fig. S4. Tio does not use ubiquitination, lysosomal degradation, or cIAP1 or cIAP2 activity to reduce the abundance of TRAF3.
- Fig. S5. Quantification of the extent of processing of p100 to p52 in the presence of combinatorial Tio mutants.

Table S1. Primer sequences.

REFERENCES AND NOTES

- S. Vallabhapurapu, M. Karin, Regulation and function of NF-κB transcription factors in the immune system. *Annu. Rev. Immunol.* 27, 693–733 (2009).
- L. M. Staudt, Oncogenic activation of NF-κB. Cold Spring Harb. Perspect. Biol. 2, a000109 (2010).
- P. J. Jost, J. Ruland, Aberrant NF-κB signaling in lymphoma: Mechanisms, consequences, and therapeutic implications. *Blood* 109, 2700–2707 (2007).
- D. E. de Oliveira, G. Ballon, E. Cesarman, NF-xB signaling modulation by EBV and KSHV. *Trends Microbiol.* 18, 248–257 (2010).
- K. T. Jeang, HTLV-1 and adult T-cell leukemia: Insights into viral transformation of cells 30 years after virus discovery. J. Formos. Med. Assoc. 109, 688–693 (2010).
- A. Kieser, Pursuing different 'TRADDes': TRADD signaling induced by TNF-receptor 1 and the Epstein-Barr virus oncoprotein LMP1. Biol. Chem. 389, 1261–1271 (2008).
- S. Vallabhapurapu, A. Matsuzawa, W. Zhang, P. H. Tseng, J. J. Keats, H. Wang, D. A. A. Vignali, P. L. Bergsagel, M. Karin, Nonredundant and complementary functions of TRAF2 and TRAF3 in a ubiquitination cascade that activates NIK-dependent alternative NF-κB signaling. *Nat. Immunol.* 9, 1364–1370 (2008).
- B. J. Zamegar, Y. Wang, D. J. Mahoney, P. W. Dempsey, H. H. Cheung, J. He, T. Shiba, X. Yang, W. C. Yeh, T. W. Mak, R. G. Korneluk, G. Cheng, Noncanonical NF-κB activation requires coordinated assembly of a regulatory complex of the adaptors cIAP1, cIAP2, TRAF2 and TRAF3 and the kinase NIK. Nat. Immunol. 9, 1371–1378 (2008).
- J. E. Vince, D. Chau, B. Callus, W. W. Wong, C. J. Hawkins, P. Schneider, M. McKinlay, C. A. Benetatos, S. M. Condon, S. K. Chunduru, G. Yeoh, R. Brink, D. L. Vaux, J. Silke, TWEAK-FN14 signaling induces lysosomal degradation of a cIAP1–TRAF2 complex to sensitize tumor cells to TNFα. J. Cell Biol. 182, 171–184 (2008).
- E. Varfolomeev, T. Goncharov, H. Maecker, K. Zobel, L. G. Kömüves, K. Deshayes,
 D. Vucic, Cellular inhibitors of apoptosis are global regulators of NF-κB and MAPK activation by members of the TNF family of receptors. Sci. Signal. 5, ra22 (2012).
- B. Razani, A. D. Reichardt, G. Cheng, Non-canonical NF-κB signaling activation and regulation: Principles and perspectives. *Immunol. Rev.* 244, 44–54 (2011).
- 12. S. C. Sun, Non-canonical NF-κB signaling pathway. Cell Res. 21, 71-85 (2011).
- Y. M. Thu, A. Richmond, NF-κB inducing kinase: A key regulator in the immune system and in cancer. Cytokine Growth Factor Rev. 21, 213–226 (2010).
- H. Häcker, P. H. Tseng, M. Karin, Expanding TRAF function: TRAF3 as a tri-faced immune regulator. Nat. Rev. Immunol. 11, 457–468 (2011).
- H. Ye, Y. C. Park, M. Kreishman, E. Kieff, H. Wu, The structural basis for the recognition of diverse receptor sequences by TRAF2. Mol. Cell 4, 321–330 (1999).
- K. R. Ely, R. Kodandapani, S. Wu, Protein-protein interactions in TRAF3. Adv. Exp. Med. Biol. 597, 114–121 (2007).

- B. Zamegar, S. Yamazaki, J. Q. He, G. Cheng, Control of canonical NF-kB activation through the NIK-IKK complex pathway. *Proc. Natl. Acad. Sci. U.S.A.* 105, 3503–3508 (2008).
- Y. Sasaki, D. P. Calado, E. Derudder, B. Zhang, Y. Shimizu, F. Mackay, S. Nishikawa, K. Rajewsky, M. Schmidt-Supprian, NIK overexpression amplifies, whereas ablation of its TRAF3-binding domain replaces BAFF:BAFF-R-mediated survival signals in B cells. *Proc. Natl. Acad. Sci. U.S.A.* 105, 10883–10888 (2008).
- S. Basak, H. Kim, J. D. Kearns, V. Tergaonkar, E. O'Dea, S. L. Werner, C. A. Benedict, C. F. Ware, G. Ghosh, I. M. Verma, A. Hoffmann, A fourth IκB protein within the NF-κB signaling module. *Cell* 128, 369–381 (2007).
- J. C. Albrecht, U. Friedrich, C. Kardinal, J. Koehn, B. Fleckenstein, S. M. Feller,
 B. Biesinger, Herpesvirus ateles gene product Tio interacts with nonreceptor protein tyrosine kinases. J. Virol. 73, 4631–4639 (1999).
- S. Heinemann, B. Biesinger, B. Fleckenstein, J. C. Albrecht, NFκB signaling is induced by the oncoprotein Tio through direct interaction with TRAF6. *J. Biol. Chem.* 281, 8565–8572 (2006).
- J. C. Albrecht, I. Müller-Fleckenstein, M. Schmidt, B. Fleckenstein, B. Biesinger, Tyrosine phosphorylation of the Tio oncoprotein is essential for transformation of primary human T cells. *J. Virol.* 79, 10507–10513 (2005).
- J. C. Albrecht, B. Biesinger, I. Müller-Fleckenstein, D. Lengenfelder, M. Schmidt, B. Fleckenstein, A. Ensser, Herpesvirus ateles Tio can replace herpesvirus saimiri StpC and Tip oncoproteins in growth transformation of monkey and human T cells. J. Virol. 78, 9814–9819 (2004).
- S. J. de Jong, J. C. Albrecht, M. Schmidt, I. Müller-Fleckenstein, B. Biesinger, Activation of noncanonical NF-κB signaling by the oncoprotein Tio. *J. Biol. Chem.* 285, 16495–16503 (2010).
- S. Wu, P. Xie, K. Welsh, C. Li, C. Z. Ni, X. Zhu, J. C. Reed, A. C. Satterthwait, G. A. Bishop, K. R. Ely, LMP1 protein from the Epstein-Barr virus is a structural CD40 decoy in B lymphocytes for binding to TRAF3. J. Biol. Chem. 280, 33620–33626 (2005).
- A. Oeckinghaus, M. S. Hayden, S. Ghosh, Crosstalk in NF-κB signaling pathways. Nat. Immunol. 12, 695–708 (2011).
- S. C. Sun, P. A. Ganchi, C. Béraud, D. W. Ballard, W. C. Greene, Autoregulation of the NF-κB transactivator RelA (p65) by multiple cytoplasmic inhibitors containing ankyrin motifs. *Proc. Natl. Acad. Sci. U.S.A.* 91, 1346–1350 (1994).
- Z. B. Yilmaz, D. S. Weih, V. Sivakumar, F. Weih, RelB is required for Peyer's patch development: Differential regulation of p52–RelB by lymphotoxin and TNF. *EMBO J.* 22, 121–130 (2003).
- E. Dejardin, N. M. Droin, M. Delhase, E. Haas, Y. Cao, C. Makris, Z. W. Li, M. Karin, C. F. Ware, D. R. Green, The lymphotoxin-β receptor induces different patterns of gene expression via two NF-κB pathways. *Immunity* 17, 525–535 (2002).
- Y. N. Demchenko, O. K. Glebov, A. Zingone, J. J. Keats, P. L. Bergsagel, W. M. Kuehl, Classical and/or alternative NF-κB pathway activation in multiple myeloma. *Blood* 115, 3541–3552 (2010).
- L. V. Pham, L. Fu, A. T. Tamayo, C. Bueso-Ramos, E. Drakos, F. Vega, L. J. Medeiros, R. J. Ford, Constitutive BR3 receptor signaling in diffuse, large B-cell lymphomas stabilizes nuclear factor-κB-inducing kinase while activating both canonical and alternative nuclear factor-κB pathways. *Blood* 117, 200–210 (2011).
- P. S. Norris, C. F. Ware, The LTβR signaling pathway. Adv. Exp. Med. Biol. 597, 160– 172 (2007).
- V. Soni, E. Cahir-McFarland, E. Kieff, LMP1 TRAFficking activates growth and survival pathways. Adv. Exp. Med. Biol. 597, 173–187 (2007).
- J. M. Zapata, V. Martínez-García, S. Lefebvre, Phylogeny of the TRAF/MATH domain. Adv. Exp. Med. Biol. 597, 1–24 (2007).
- C. Z. Ni, G. Oganesyan, K. Welsh, X. Zhu, J. C. Reed, A. C. Satterthwait, G. Cheng, K. R. Ely, Key molecular contacts promote recognition of the BAFF receptor by TNF receptor-associated factor 3: Implications for intracellular signaling regulation. *J. Immunol.* 173, 7394–7400 (2004).
- S. C. Sun, Controlling the fate of NIK: A central stage in noncanonical NF-κB signaling. Sci. Signal. 3, pe18 (2010).
- G. Liao, M. Zhang, E. W. Harhaj, S. C. Sun, Regulation of the NF-κB-inducing kinase by tumor necrosis factor receptor-associated factor 3-induced degradation. *J. Biol. Chem.* 279, 26243–26250 (2004).
- H. Sanjo, D. M. Zajonc, R. Braden, P. S. Norris, C. F. Ware, Allosteric regulation of the ubiquitin:NIK and ubiquitin:TRAF3 E3 ligases by the lymphotoxin-β receptor. *J. Biol. Chem.* 285, 17148–17155 (2010).
- A. Kieser, C. Kaiser, W. Hammerschmidt, LMP1 signal transduction differs substantially from TNF receptor 1 signaling in the molecular functions of TRADD and TRAF2. EMBO J. 18. 2511–2521 (1999).
- K. Katsch, S. J. de Jong, M. Schmidt, I. Müller-Fleckenstein, B. Fleckenstein, J. C. Albrecht,
 B. Biesinger, Species restriction of *Herpesvirus saimiri* and *Herpesvirus ateles*: Human lymphocyte transformation correlates with distinct signaling properties of viral oncoproteins. *Virus Res.* 165, 179–189 (2012).
- J. S. Bonifacino, Metabolic labeling with amino acids. Curr. Protoc. Cell Biol. Chapter 7, Unit 7.1 (2001).

RESEARCH ARTICLE

- K. Heinzelmann, B. A. Scholz, A. Nowak, E. Fossum, E. Kremmer, J. Haas, R. Frank, B. Kempkes, Kaposi's sarcoma-associated herpesvirus viral interferon regulatory factor 4 (vIRF4/K10) is a novel interaction partner of CSL/CBF1, the major downstream effector of Notch signaling. *J. Virol.* 84, 12255–12264 (2010).
- H. R. Lee, W. C. Choi, S. Lee, J. Hwang, E. Hwang, K. Guchhait, J. Haas, Z. Toth, Y. H. Jeon, T. K. Oh, M. H. Kim, J. U. Jung, Bilateral inhibition of HAUSP deubiquitinase by a viral interferon regulatory factor protein. *Nat. Struct. Mol. Biol.* 18, 1336–1344 (2011).
- N. Eswar, D. Eramian, B. Webb, M. Y. Shen, A. Sali, Protein structure modeling with MODELLER. *Methods Mol. Biol.* 426, 145–159 (2008).
- A. C. Wallace, R. A. Laskowski, J. M. Thornton, LIGPLOT: A program to generate schematic diagrams of protein-ligand interactions. *Protein Eng.* 8, 127–134 (1995).
- R. A. Sayle, E. J. Milner-White, RASMOL: Biomolecular graphics for all. *Trends Biochem. Sci.* 20, 374 (1995).
- J. D. Thompson, T. J. Gibson, D. G. Higgins, Multiple sequence alignment using ClustalW and ClustalX. Curr. Protoc. Bioinformatics Chapter 2, Unit 2.3 (2002).

Acknowledgments: We thank M. Schmidt and I. Müller-Fleckenstein for transformed cell cultures and B. Fleckenstein for valuable suggestions. LBW242 was a gift of Novartis Pharma AG (Basel). Funding: This work was supported by grants from the German Research Foundation (Bl465/5-1, GRK1071/C3) to B.B., the Elite Network of Bavaria (BIGSS) and the Friedrich-Alexander-Universität Erlangen-Nürnberg (FFL) to S.J.d.J., SFB796 (project A2) to H.S., and SFB 684 (project A20) and the LifeScience Foundation to A.K. Author contributions: S.J.d.J., A.K., H.S., and B.B. planned the experiments; S.J.d.J., J.-C.A., F.G., H.S., and B.B. performed the experiments; and S.J.d.J., H.S., and B.B. wrote the manuscript. Competing interests: The authors declare that they have no competing interests.

Submitted 14 June 2012 Accepted 5 April 2013 Final Publication 23 April 2013 10.1126/scisignal.2003309

Citation: S. J. de Jong, J.-C. Albrecht, F. Giehler, A. Kieser, H. Sticht, B. Biesinger, Noncanonical NF- κ B activation by the oncoprotein Tio occurs through a nonconserved TRAF3-binding motif. *Sci. Signal.* **6**, ra27 (2013).